

Surface Patterns in Temperature, Flow, Phytoplankton Biomass, and Species Composition in the Coastal Transition Zone off Northern California

RALEIGH R. HOOD¹

Scripps Institution of Oceanography, University of *California*, San *Diego*, La Jolla

MARK R. ABBOTT, ADRIANA HUYER, AND P. MICHAEL KOSRO

College of Oceanography, Oregon State University, Corvallis

Satellite thermal imagery and in situ biological and physical data are presented that describe the spatial variability of phytoplankton biomass and species composition in relation to the physical structure at the sea surface during persistent upwelling off northern California. Surface patterns in temperature, geostrophic velocity, chlorophyll, and particle size structure show that the coastal zone was dominated by two water masses separated by a well-defined physical boundary. This boundary is apparent in satellite thermal imagery as a cold front and in dynamic height as a meandering jet in the California Current. On the landward side of the front (jet) we observed cold, coastal water that was relatively enriched in phytoplankton biomass, due to the presence of large diatoms. On the seaward side of the front (jet) we observed relatively warm water where the phytoplankton biomass was low and the diatoms were largely absent. Broad tongues and narrow filaments of cold, chlorophyll-rich water that extended over 100 km offshore were present in our study area. These features were bounded by the meandering coastal jet. The coldest, most chlorophyll-rich water in these tongues and filaments was located between the onshore and offshore flows in relatively slow moving water, but entrainment of coastal water into the jet was apparent.

INTRODUCTION

Satellite data has dramatically changed our view of physical and biological processes in the upper ocean. This is especially true of the more dynamic ocean regions like the Gulf Stream and California Current system (CCS). Thermal and color imagery has revealed complex patterns in both flow and phytoplankton biomass that were previously unresolved by shipboard data. Our view of these dynamic oceanic regions has changed from one of broad uniform flows with gradual biological gradients, to one of narrow, rapid flows characterized by mesoscale meander and eddy structures which transport plankters in complex ways.

In eastern ocean boundary currents, like the CCS, wind-driven coastal upwelling adds another dimension of complexity to the physical and biological fields. The relative importance of zonal (offshore transport of upwelled water) and meridional (southward transport of water from high latitudes) contributions to production in the CCS is a subject of debate. The traditional view holds that production at all trophic levels in the CCS is supported primarily by both nutrients and plankton biomass advected southward from higher latitudes. This view originated from large time and space scale studies of the CCS carried out by California Cooperative Oceanic Fisheries Investigations (CalCOFI), which show meridional continuity of both flow and zooplankton biomass, and a zooplankton biomass maximum that is farther offshore than expected if coastal upwelling were supporting it [Wyllie, 1966; Smith, 1971]. Correlation

analyses have shown that zooplankton biomass offshore in the CCS is more closely related to southward transport than it is to coastal upwelling indices [Chelton et al., 1982]. However, recent satellite studies of the CCS have challenged this traditional view [Mooers and Robinson, 1984; Rienecker et al., 1985]. During persistent upwelling periods off northern California (e.g. the late spring and early summer months) narrow (< 50 km wide) tongues of cold chlorophyll-rich water ("filaments") are commonly observed which extend hundreds of kilometers offshore from the coast into the outer reaches of the California Current System [Breaker and Gilliland, 1981; Traganza et al., 1981; Abbott and Zion, 1985; Davis, 1985; Flament et al., 1985; Kosro and Huyer, 1986]. It has been hypothesized that these features represent regions of seaward transport of nutrients and plankton biomass from the coastal zone, and that this transport contributes significantly to production offshore. Estimates of transport in these offshore flows are on the order of 1 to 2 Sverdrups, which is about 20 percent of the climatological mean California Current [Mooers and Robinson, 1984].

Satellite images give the impression that filaments represent narrow and relatively uniform seaward flows imbedded in a mesoscale eddy field. Filaments which terminate in dipole eddy pairs ("hammerhead structures") appear to be regions where upwelled coastal water is squirted directly offshore. However, combined satellite and in situ studies of the northern California coastal region have now shown that the cold filaments we see in satellite images are the result of entrainment of coastal water into narrow (< 50 km wide) seaward flows ("jets") in the CCS [Flament et al., 1985; Rienecker and Mooers, 1989]. These jets appear to be part of much larger scale meandering southward flows in the CCS [Wyllie, 1966; Ikeda and Emery, 1984]. When meanders impinge upon the coast, cold water is entrained and then advected seaward as the flow turns offshore. Thus, the quantity of coastal water transported offshore represents some fraction of the total jet transport. That is, it appears

¹Now at College of Oceanography, Oregon State University, Corvallis.

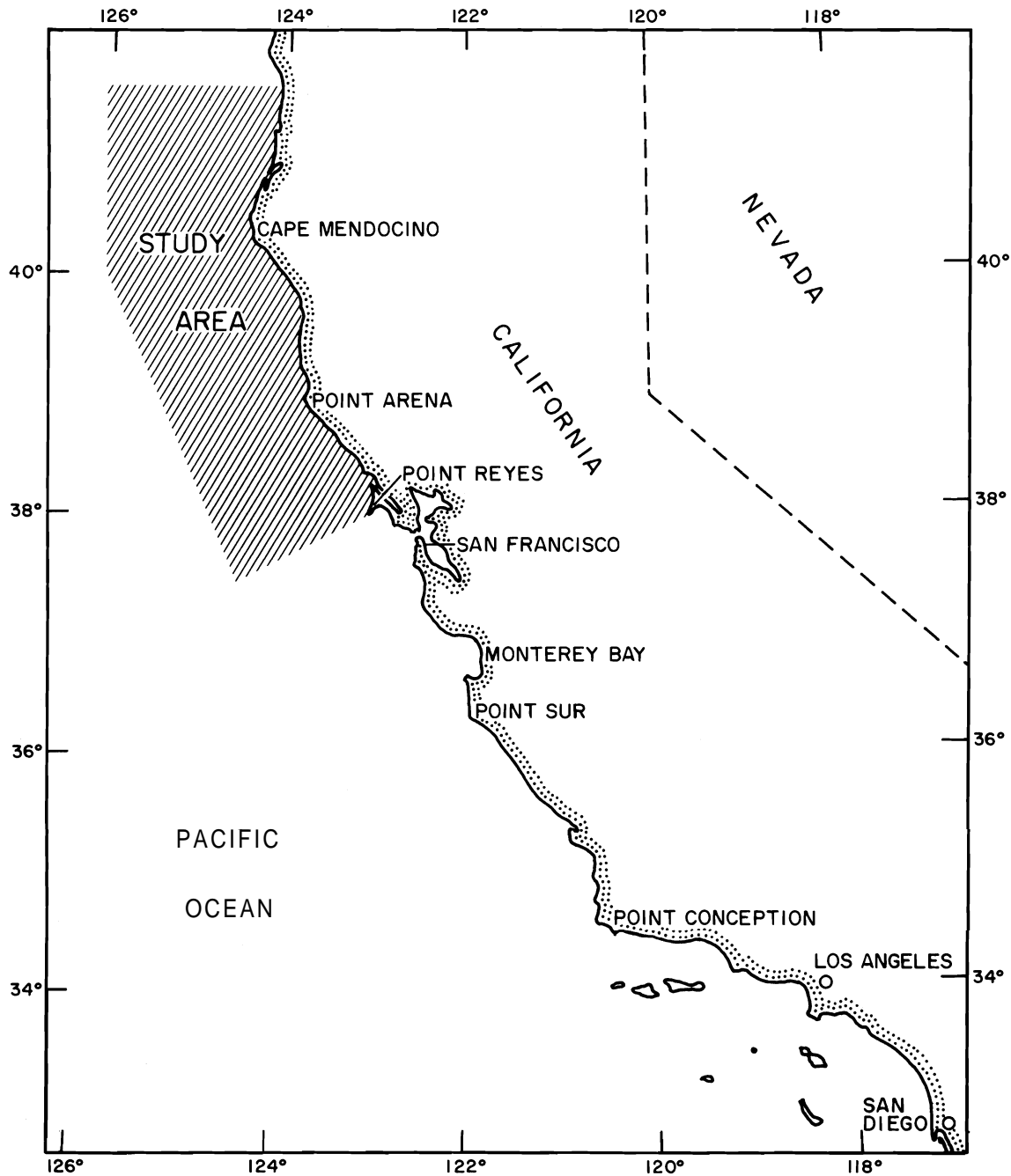


Fig. 1. The California coastline and the coastal transition zone study area for the 1987 cruises.

that the filaments themselves do not represent 1 to 2 Sverdrup flows, but some fraction of it.

In this paper we present physical and biological data collected from the coastal transition zone (between 50 and 150 km from the coast) off northern California during a period of persistent upwelling. We describe patterns in surface temperature and flow in relation to distributions of phytoplankton biomass and species composition in a region where tongues and filaments of coastal water extended a few hundreds of kilometers offshore. Our data show that these seaward extensions of cold water were associated with variations in the offshore position of a thermal front which was

associated with meanders in a well-defined jet in the CCS, and we show evidence of entrainment and downstream advection of coastal phytoplankters in the meandering flow.

STUDY AREA AND METHODS

These data were collected on a 10-day cruise in June (9–19) of 1987 on the R. V. *Wecoma*. We sampled a station grid that extended from Point Reyes to just north of Cape Mendocino (Figures 1 and 3). This survey was intended to cover the transition zone between cold, freshly upwelled water near the coast, and warm, oceanic water offshore. CTD

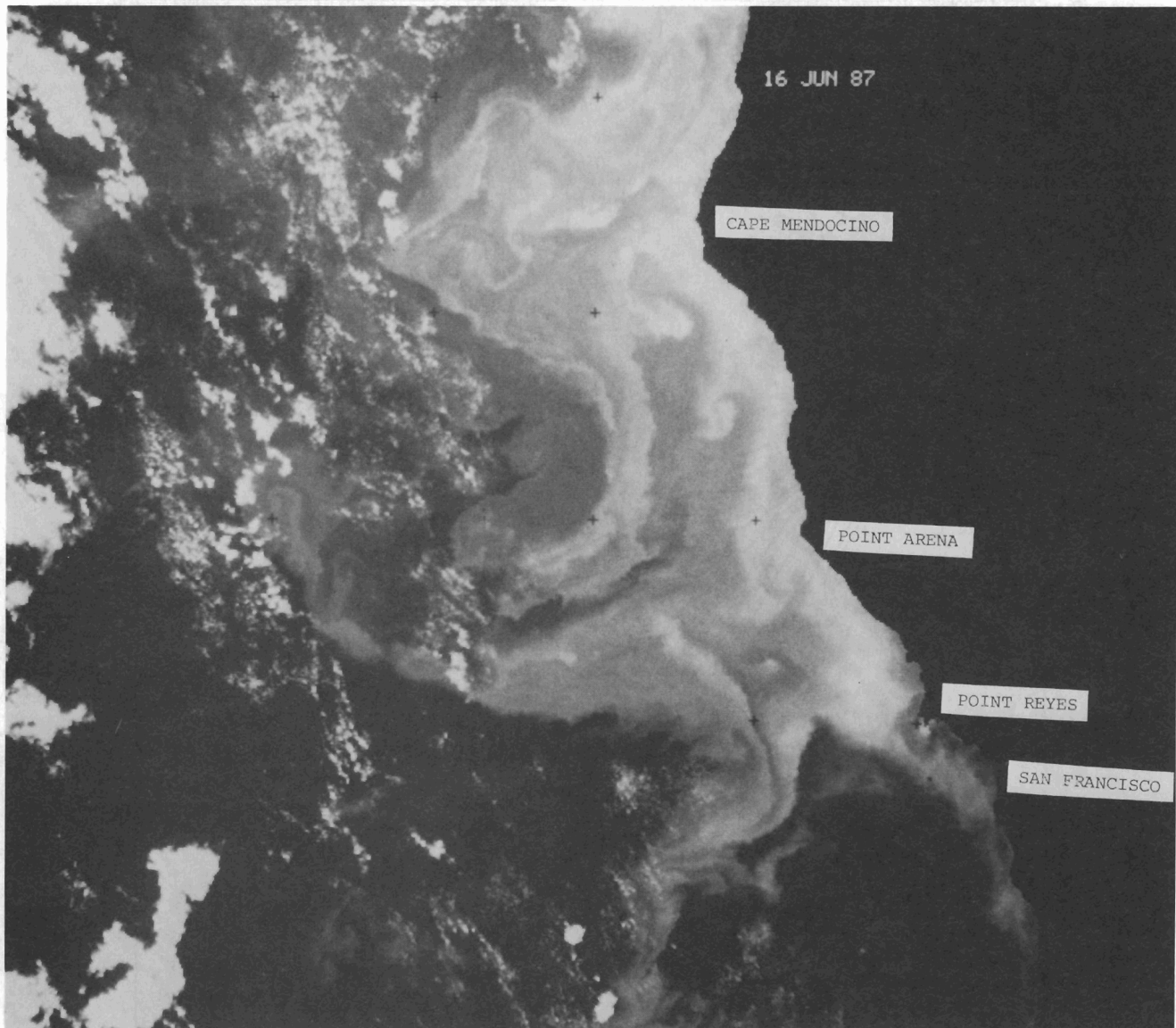


Fig. 2. A satellite AVHRR thermal image of the northern California coastal region collected on June 16, 1987. The light grey shades represent cold water.

casts were made to 500 m, acoustic Doppler current profiles (ADCP) were collected continuously, and discrete depths were sampled for chemical and biological analyses. The data presented here include satellite sea surface temperature, in situ sea surface temperature, dynamic height, ADCP velocity, chlorophyll-a concentration, particle size spectra, and photomicrographs showing phytoplankton species composition.

Satellite thermal (AVHRR) imagery was collected and processed at the Scripps Satellite Oceanography Facility. The data were geographically corrected, calibrated to infrared brightness temperature, and linearly mapped to grey shades to give relative values of surface temperature. Geophysical algorithms for deriving absolute temperatures were not applied.

CTD observations were made with a Neil Brown Mark IIIb CTD system. The probe was calibrated for pressure, temperature, and conductivity by the manufacturer, and the

temperature and conductivity data were checked against in situ calibration samples. The geopotential anomaly (dynamic height) was calculated from the equation of state of seawater using standard algorithms [Schramm et al., 1988]. A 300-kHz acoustic Doppler current profiler manufactured by RD Instruments was used in conjunction with a Northstar LORAN-C to estimate near-surface currents following procedures described by Kosro [1985].

Chlorophyll-a samples were filtered (Whatman GF/F), frozen, and stored for subsequent laboratory analysis. Concentration was determined fluorometrically after 24-hour extraction in 90% acetone. Particle concentration and size spectra between 4 and 100 μm equivalent spherical diameter (E.S.D.) were measured at sea using a Coulter Electronics particle analyzer equipped with a 280- μm aperture. The samples were prefiltered through a 295- μm sieve to prevent clogging. Phytoplankton samples were preserved in 2% buffered formalin and stored for microscopic analysis. In

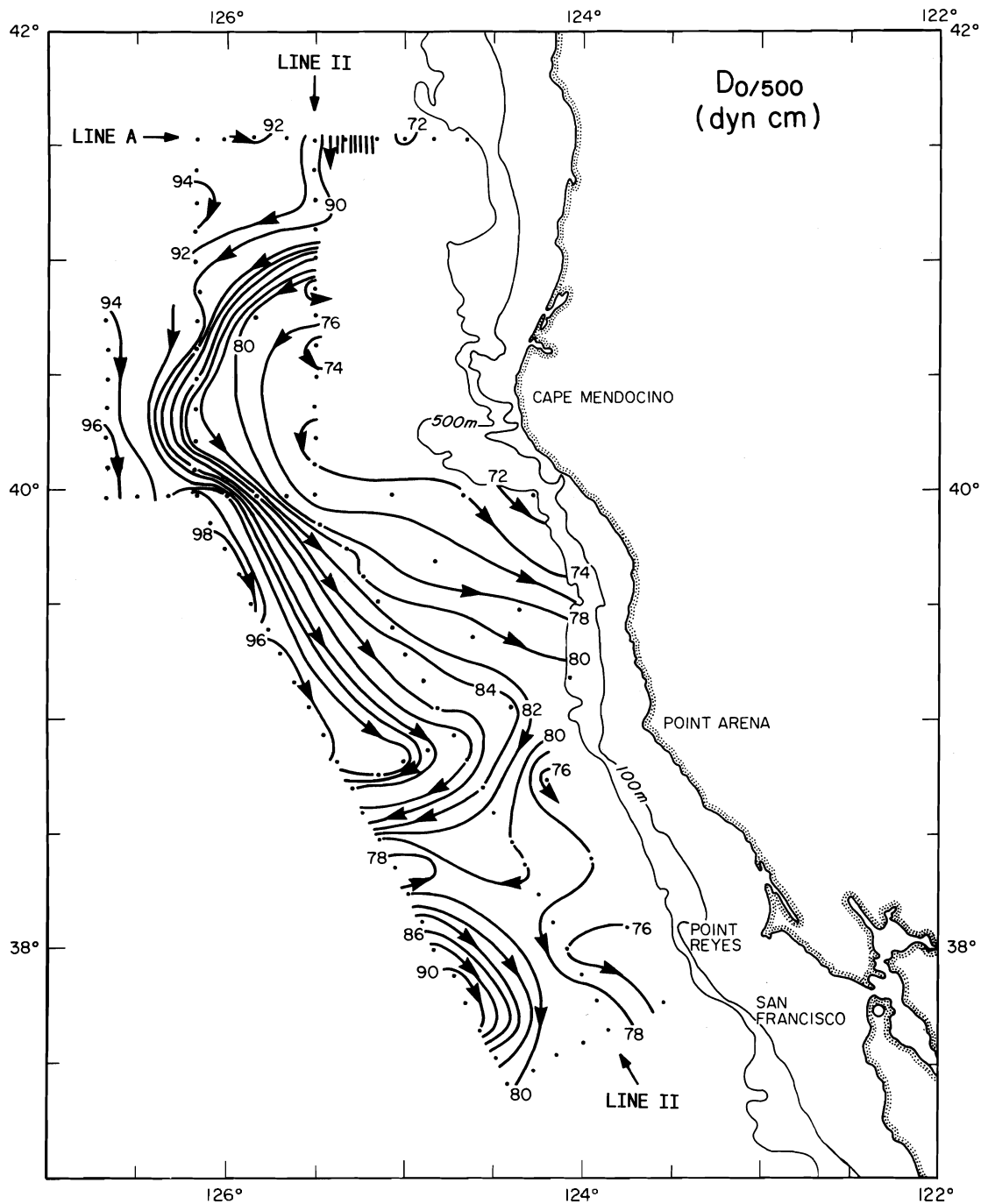


Fig. 3. The geopotential anomaly at the sea surface relative to 500 dbar. Streamlines indicate the direction and intensity of the flow.

the laboratory 50-mL aliquots were settled and examined to identify the dominant phytoplankters.

RESULTS

Surface Distributions of Temperature and Geostrophic Flow

Winds were generally strong and favorable for upwelling in May and June of 1987. The shipboard measurements showed that the winds were consistently directed southeastward (alongshore) during our cruise, with a mean velocity of 9.8 m s^{-1} and a range of 4 to 18.5 m s^{-1} [Schramm et al., 1988]. Figure 2 is a satellite AVHRR image of surface

temperature collected on June 16. It covers most of the coastal zone between Monterey Bay and California/Oregon border. Although this image was collected near the end of the cruise it is fairly representative of the near-surface thermal pattern throughout the sampling period. The light grey shades show a broad heterogeneous region of cold water along the coast from the California/Oregon border to Point Reyes, and the dark grey shades show warmer water offshore. The boundary between cold, coastal water and warm, oceanic water defines a thermal front that was generally situated between 50 and 150 km from the coast. North of Cape Mendocino this front was relatively close to the

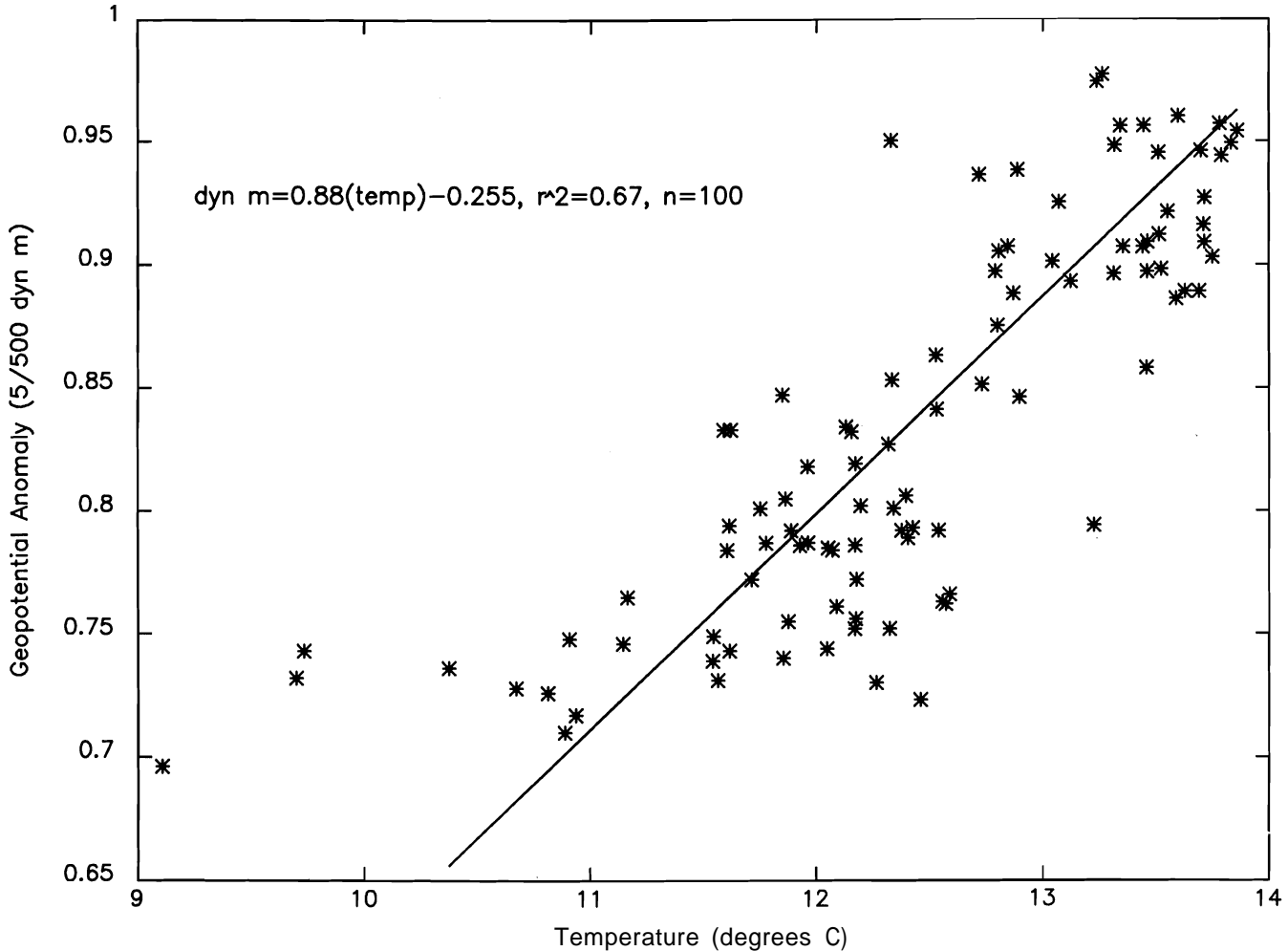


Fig. 4. The relationship between in situ near-surface (5 m) temperature and the geopotential anomaly at the sea surface relative to 500 dbar. The line was fit by eye to the main trend in the data.

shore, and it extended seaward about 150 km directly off Cape Mendocino. This front swung landward again south of Cape Mendocino, and it defined two cold water filaments off Point Arena and Point Reyes. One of these filaments extended seaward and northward, terminating in a pool of cool water 280 km off Point Arena, and the other extended seaward and southward, passing about 220 km off Monterey Bay.

Figure 3 is a plot of the geopotential anomaly at the sea surface relative to 500 m. These data show that the sea surface height was generally low nearshore and high offshore. The transition between these two regimes was rather abrupt and thus defined a meandering geostrophic jet. This jet, which is approximately bounded by the 80 and 90 dyn cm contours in Figure 3, meandered generally southward between 50 and 150 km from shore. It flowed south into our study area across the northern-most station line and then took an abrupt seaward turn north off Cape Mendocino. Off Cape Mendocino the current meandered seaward, and then flowed southeastward toward shore. The jet took another sharp seaward turn off Point Arena and flowed out of our study area, and off Point Reyes it flowed back into our study area and then turned seaward once again. The dynamic topography showed good agreement with Doppler acous-

tic current measurements [Coastal Transition Zone Group, 1988] which indicates that the currents were approximately geostrophic. Near-surface ADCP velocities were on the order of 50 cm s^{-1} in the meander off Cape Mendocino and 70 cm s^{-1} off Point Arena and Point Reyes.

A comparison of Figures 2 and 3 reveals an obvious similarity in the temperature and flow patterns. That is, the temperature front, which separated the cold, coastal water from the warmer, oceanic water in Figure 2, was generally coincident with the current jet which dominated the geostrophic flow field in Figure 3. Where the temperature front extended seaward off Cape Mendocino the near-surface jet took a broad seaward meander, and the filament of cold water which extended seaward off Point Arena was sandwiched by a seaward jet to the north and a return flow to the south. Thus, the cold tongues and filaments apparent in the satellite imagery were generally bounded by a meandering coastal jet. In Figure 4, in situ near-surface temperature is plotted against the geopotential anomaly (5/500). With the exception of a few of the low values, this relationship is fairly linear ($\text{dyn m} = 0.88(\text{temp}) - 0.255$, $r^2 = 0.67$, $n = 100$). That is, where the surface water was cold the dynamic height was low and where the surface water was warm the dynamic height was high. If we use the 0.8 and 0.9 dyn m contours to

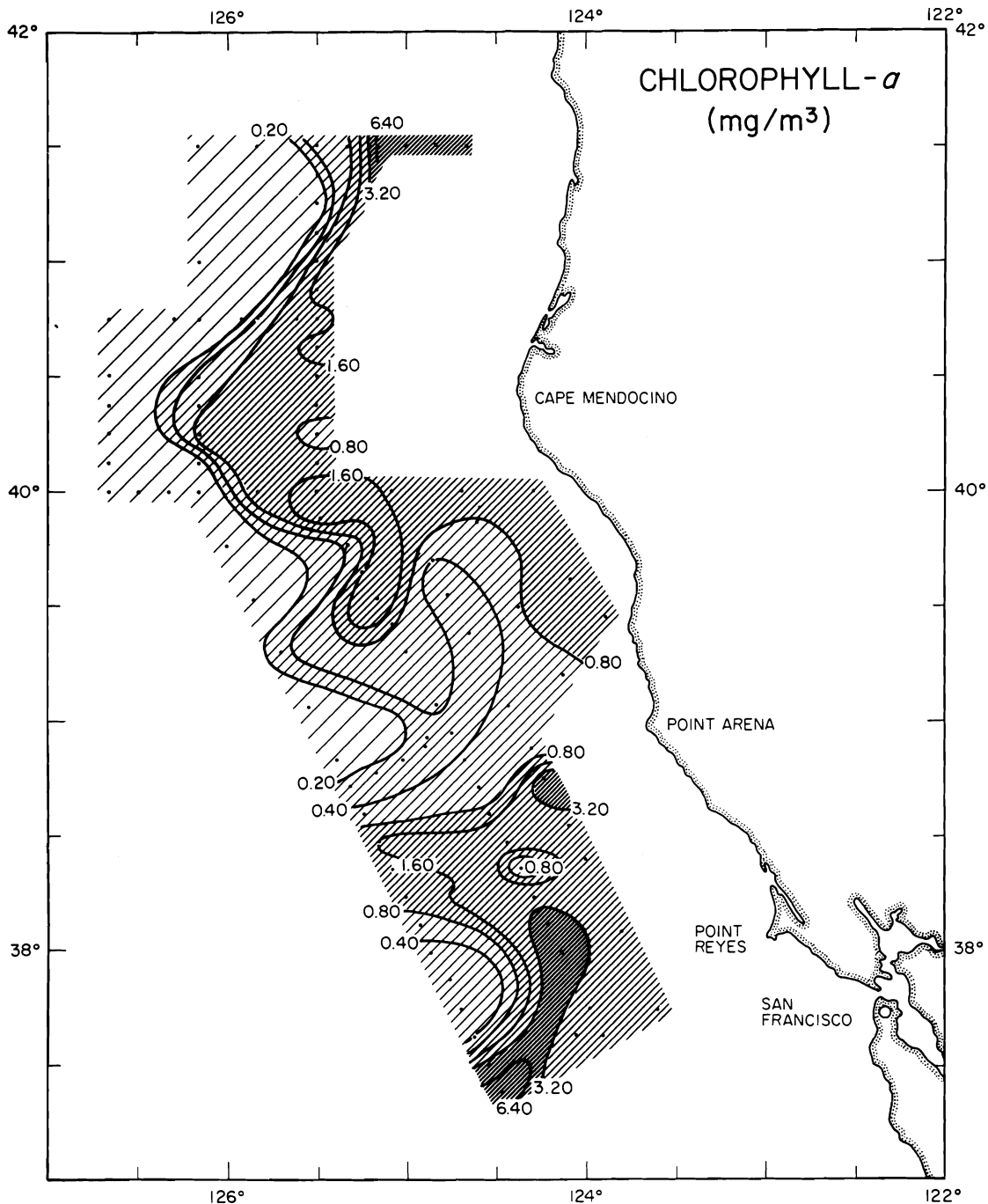


Fig. 5. The near-surface (5 m) distribution of chlorophyll-a.

define the boundaries of the jet, it is apparent that the region of rapid flow separated warm surface water on its high side (in terms of dynamic height) from cold surface water on its low side, and the jet itself encompassed a broad range of temperatures (≈ 11.5 to 13.75°C).

Surface Distributions of Chlorophyll and Particle Volume in Relation to Temperature and Flow

The surface distribution of phytoplankton biomass is depicted in Figures 5 and 6 as chlorophyll-a concentration and particle volume concentration, respectively. The latter was calculated from the electronic particle analyzer data by sum-

ming the particle volume in each size class between 4 and $100\ \mu\text{m}$ E.S.D. The patterns in these two plots are similar. They both depict a patchy distribution of biomass that was higher toward shore and lower offshore. On the northernmost station line, high values of chlorophyll and particle volume were located toward shore north of Cape Mendocino, and moderate values extended seaward in a broad tongue directly off Cape Mendocino. Patches of high chlorophyll and particle volume were located to the southwest of Cape Mendocino which protruded seaward between Cape Mendocino and Point Arena. Just south of this patch the phytoplankton biomass was relatively low except very near the coast. In the southern portion of the study area, the chlorophyll and par-

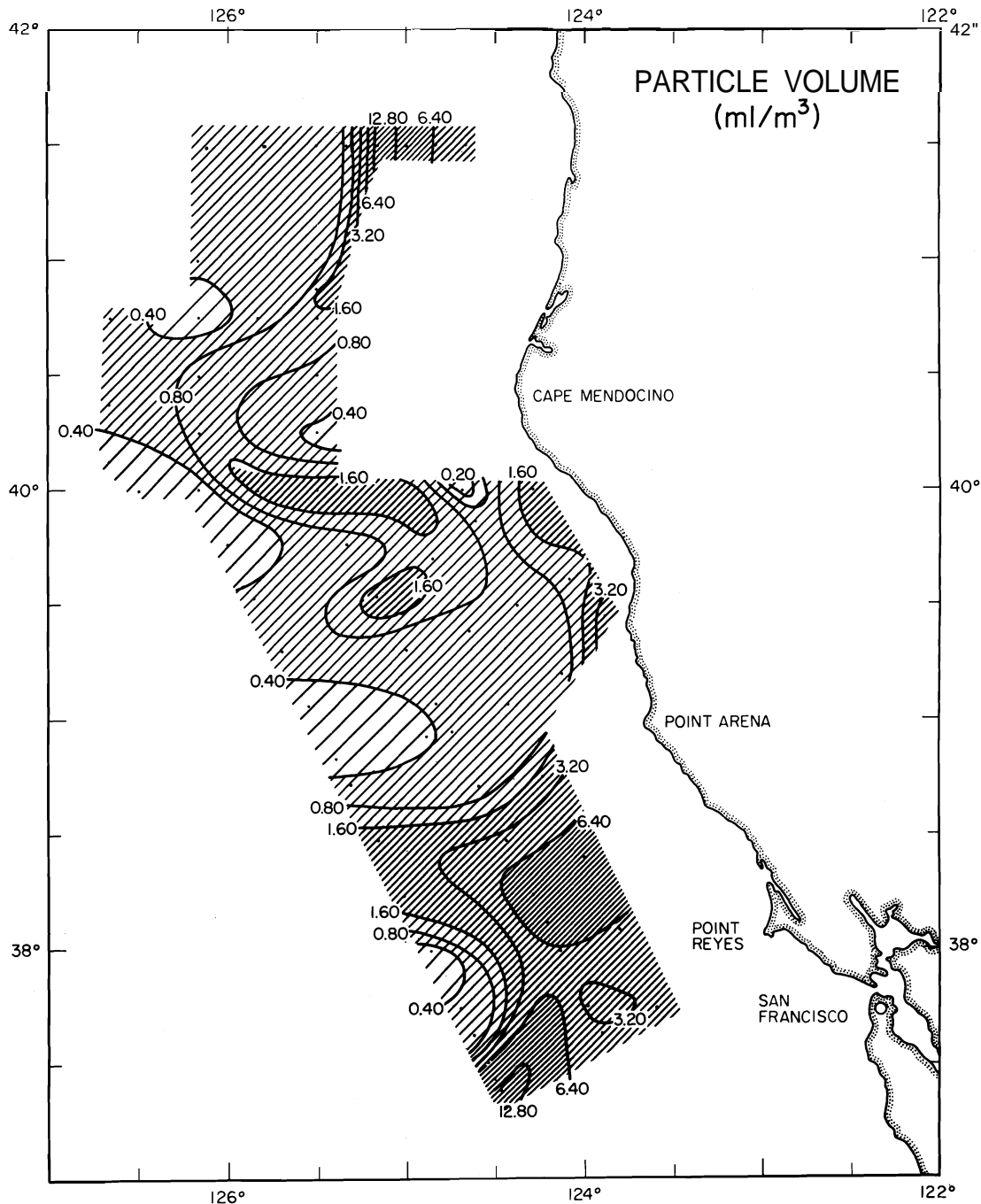


Fig. 6. The near-surface (5 m) distribution of estimated particle volume between 4 and 100 μm .

ticle volume concentrations were generally high and patchy, and both plots depict two seaward extensions of high phytoplankton biomass, one off Point Arena and one off Point Reyes.

A comparison of our surface maps of chlorophyll and particle volume (Figures 5 and 6) with the satellite thermal imagery (Figure 2) and the geopotential anomaly (Figure 3) reveals that the patterns in temperature, sea surface height, and phytoplankton biomass are similar. In general, the chlorophyll and particle volume concentrations were higher in the cold water where the sea surface height was low, and lower in the warm water where the sea surface height was

high. The transition between these two biological zones was generally coincident with the temperature front and the geostrophic jet apparent in Figures 2 and 3. Where the front (jet) extended seaward, the high phytoplankton biomass extended seaward as well. Off Cape Mendocino the front (jet) defined the boundary of a broad seaward extension of cold, chlorophyll-rich water, and the filament of cold, chlorophyll-rich water that extended seaward off Point Arena was bounded by this front (jet) to the north and south. In Figure 7 the chlorophyll-a concentration is plotted on a logarithmic scale against dynamic height ($5/500$). The data points define a line which describes a decrease in

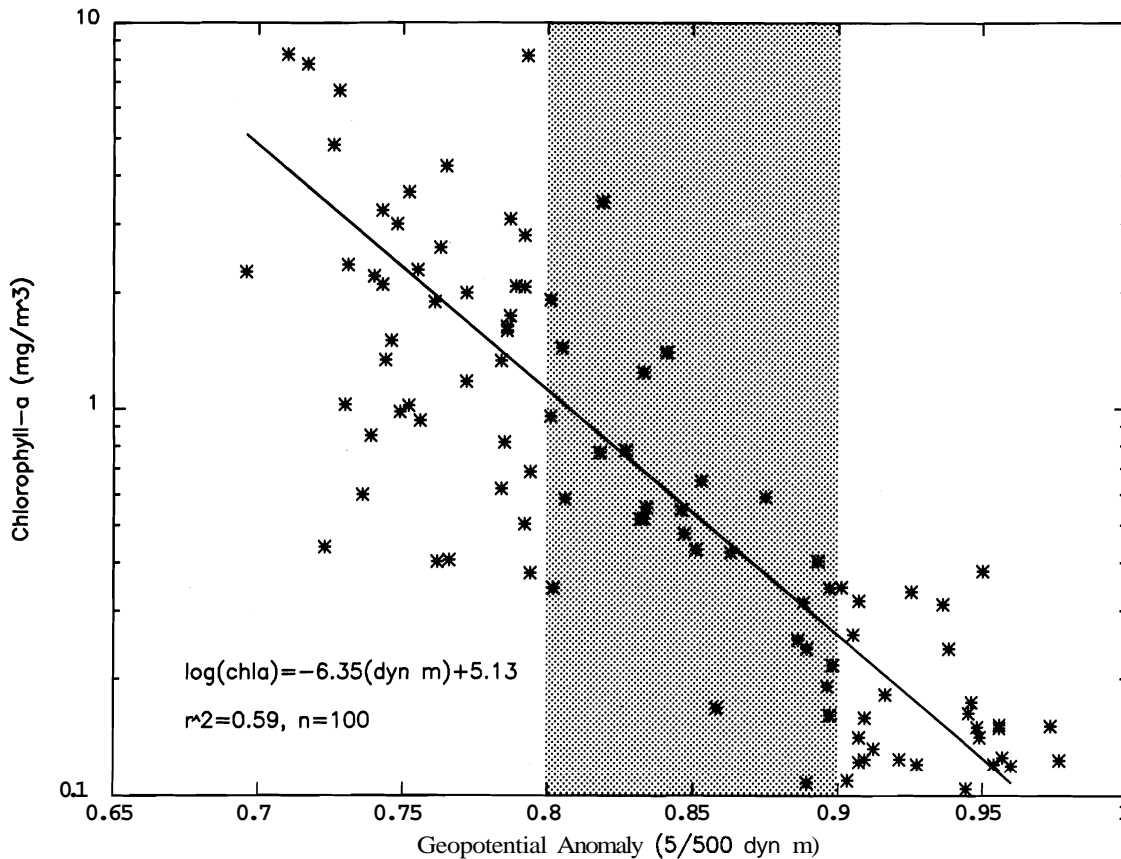


Fig. 7. The relationship between the geopotential anomaly at the sea surface relative to 500 dbar and the near-surface (5 m) chlorophyll-a concentration. The line was fit by eye to the main trend in the data. The grey-shaded region shows the approximate location of the geostrophic jet and the chlorophyll concentrations it enveloped.

chlorophyll concentration with increasing sea surface height ($\log(\text{chla}) = -6.35(\text{dyn m}) + 5.13$, $r^2 = 0.59$, $n = 100$). That is, the main trend in the data is an exponential increase in the chlorophyll concentration with decreasing sea surface height. Again, if we define the geostrophic jet by the 0.8 and 0.9 dyn m contours (greyshaded region) we see that it was associated with the transition between lower and less variable chlorophyll concentrations on its high side and higher and more variable chlorophyll concentrations on its low side. The jet itself encompassed a broad range of chlorophyll concentrations (? 0.1 to 3 mg m^{-3}).

In Figure 8, we have plotted chlorophyll-a concentration against the eastward component of the nearsurface velocity (approximately 20 m depth) estimated with the acoustic Doppler current profiler. These data show that the range of chlorophyll values varied strongly with the magnitude of the zonal flow. In regions where the zonal flow was rapid, the chlorophyll values were generally lower, and where the zonal flow was slow, the range of chlorophyll values was large. The distribution of data points about zero is approximately symmetric.

Particle Size Spectra and Phytoplankton Species Composition in Relation to the Front (Jet)

Figure 9 is a three-dimensional plot of particle size (4 – 100 μm E.S.D.) versus particle volume along the north-

ernmost zonal station line (line A, Figure 3). Station 91 was furthest offshore and station 126 was furthest inshore. The arrow in Figure 9 indicates where the temperature front and the southward flowing jet crossed this line. This plot shows a broad distribution of relatively large particles (>20 μm E.S.D.) landward of the front (jet) (stations 123–126). This distribution represents a dense community of intermediate sized, chain-forming diatoms (Figure 11, frames 1 and 2) that was dominated by several *Chaetoceros* species and *Skeletonema costatum*. As the front (jet) was crossed between stations 87 and 123 the particle size structure changed abruptly. The large particles largely disappeared. Seaward of station 122 the phytoplankton community was dominated by small (<20 μm E.S.D.) particles that did not constitute a large volume. These particles included small pennate diatoms, flagellates, coccolithophores, dinoflagellates, and unidentifiable particulates (Figure 11, frames 3 and 4).

Figure 10 is a three-dimensional particle data plot which shows variations in the size spectra along station line II, which ran parallel to the coast about 90 km from shore (see Figure 3). Station 87 was at the northernmost end of the line off the coast north of Cape Mendocino, and station 26 was at the southernmost end of the line off Point Reyes. This transect intersected the previous transect (Figure 9) at station 87. The position the front (jet) relative to this transect is indicated by grey-shaded arrows in this figure also. The temperature front and the westward flowing surface jet

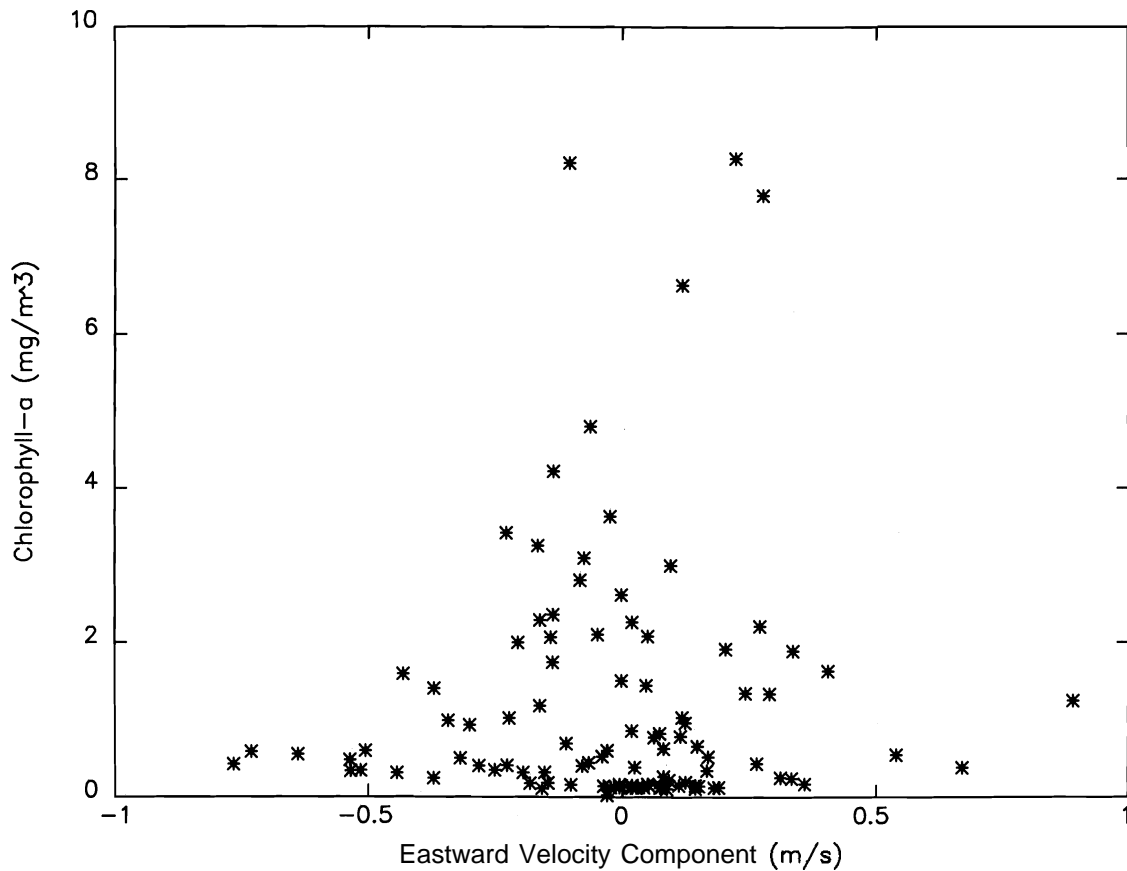


Fig. 8. The relationship between the eastward velocity component at 20 m estimated with the acoustic Doppler current profiler and the near-surface (5 m) chlorophyll-a concentration.

crossed this line between stations 81 and 85 in the north. Across the jet there was a small increase in the particle volume in the larger size classes ($>20 \mu\text{m}$ E.S.D.). The area between stations 81 and 77 was dominated by the diatom *Rhizosolenia alata* (Figure 11, frames 5 and 6). These long ($>200 \mu\text{m}$), cylindrical cells formed chains that sometimes exceeded a millimeter in length. As a result, the species was largely removed by prefiltering and it is not very well represented in the particle data. Increases in the volume of large particles were found at stations 71 and 75. Station 75 was located on the landward edge of the front (jet), and station 71 was located in the frontal region within the southward flow. These broad distributions represent patches of intermediate sized, chain-forming diatoms that were dominated by *Chaetoceros* spp. and *Skeletonema costatum*. *Rhizosolenia alata* was abundant at these stations as well (Figure 11, frames 7 and 8). Between stations 71 and 35, where the transect gradually crossed the front and the jet, large particles disappeared once again and the phytoplankton community was dominated by small ($<20 \mu\text{m}$ E.S.D.) particles that did not constitute a very large volume. As in the offshore portion of the northern zonal transect (Figure 9), these small particles included small pennate diatoms, flagellates, coccolithophores, dinoflagellates and unidentifiable particulates (Figure 12, frames 1, 2, and 3).

The temperature front and the surface jet crossed the transect in Figure 10 again between stations 33 and 37, approximately. This is where the front (jet) extended seaward off Point Arena. As the jet was crossed the parti-

cle volume increased dramatically forming a series of peaks in the large size classes ($>20 \mu\text{m}$ E.S.D.). Variations in the shape of the distributions correspond to major shifts in the dominant phytoplankters. The tall, narrow peak between stations 31 and 35 was caused by a dense population of large ($30 - 60 \mu\text{m}$ diameter), discoid single-celled species of *Actinocyclus* (*A. curvatulus* and *A. ehrenbergii*, Figure 12, frames 4 and 5). *Rhizosolenia alata* was also abundant in this region. Between stations 31 and 29 the distribution widened markedly due to the appearance of a several intermediate sized, chain-forming diatoms. At station 30 *Chaetoceros* spp., *Skeletonema costatum*, *Nitzschia* spp., and *Thalassiosira* spp. were all abundant, and *Rhizosolenia alata* and *Actinocyclus* spp. were relatively rare (Figure 12, frame 6). South of station 29 the particle size distribution became narrow once again, and a small peak in the smaller size ranges appeared. At station 26 *Actinocyclus* spp. were very abundant, other diatom species were largely absent (Figure 12, frame 7), and there were numerous small flagellates (Figure 12, frame 8).

DISCUSSION

The distribution and offshore extent of cold water shown in our satellite image (Figure 2) is fairly typical for this northern California region during the upwelling season. Maps of the mean AVHRR sea surface temperature field [Kelly, 1985] depict a cold region along the coast that is separated from warmer water offshore by a well-defined thermal

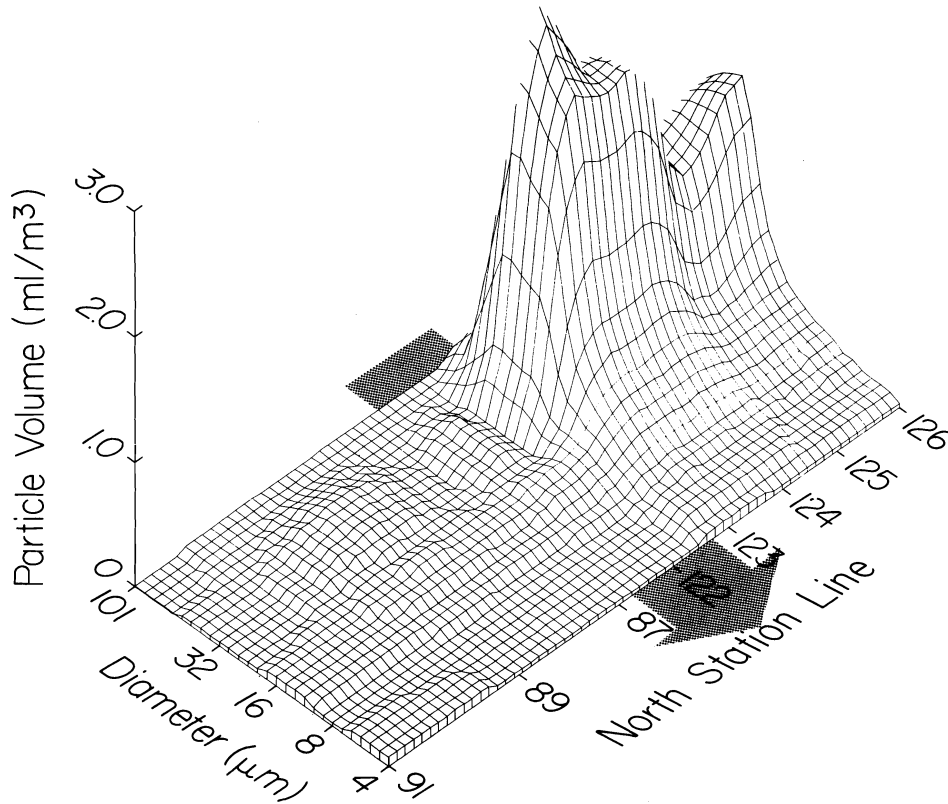


Fig. 9. An onshore/offshore transect of the near-surface (5 m) distribution of estimated particle volume as a function of estimated particle size along the northernmost station line (line A in Figure 3). The grey-shaded arrow shows the approximate location of the jet crossing.

front that extends seaward off Cape Mendocino and Point Arena. Southward meandering near-surface jets, like the one that dominates the geostrophic flow field in Figure 3, seem to be a characteristic feature of the California Current system during the upwelling season; they can be seen in the dynamic height maps in *Wyllie* [1966] and *Bernstein* et al. [1977], and in the satellite images and model results of *Ikeda* and *Emery* [1984]. The sharp seaward meander that is apparent off Point Arena in Figure 3 can be seen in a number of recent satellite, hydrographic, and drifter studies of the area [Davis, 1985; Flament et al., 1985; Rienecker et al., 1985; Kosm and Huyer, 1986], and this feature is discernable in many of the summertime maps of dynamic topography from early CalCOFI surveys (e.g. June, July 1950 and July 1952 of *Wyllie* [1966]).

The general coincidence of the thermal front in the AVHRR data (Figure 2) and the geostrophic jet (Figure 3) shows that the surface temperature seen by the satellite reflected the subsurface density field from which the geopotential anomaly was calculated. *Kelly* [1983] observed similar relationships between the surface temperature field and the flow field when she compared a relatively large number of satellite thermal images to in situ data collected during the Coastal Ocean Dynamics Experiment (CODE). *Bernstein* et al. [1977] concluded that the satellite surface temperature patterns along the entire California coastline are related to the flow field, and *Ikeda* and *Emery* [1984] assume this relationship in determining flow patterns from satellite thermal imagery.

The seaward extensions of cold, coastal water apparent in our satellite imagery were clearly related to the position

of the meandering geostrophic jet in our study area. The broad tongue of cold water that extended seaward off Cape Mendocino was bounded by the jet, and the cold filament off Point Arena was bounded to the north by an offshore flow and to the south by an onshore flow. Since most of the cold water in these features was found on the low (in terms of dynamic height) side of the meandering flow, and not in the flow itself, we suspect that there was an important vertical contribution of cold water (upwelling), perhaps associated with the geostrophic adjustment in the jet.

The large-scale distributions of temperature (Figure 2) and phytoplankton biomass (Figures 5 and 6) were similar because the colder water supported a higher biomass of various diatom species (e.g., *Rhizosolenia alata*, *Skeletonema costatum*, *Actinocyclus* spp., and *Chaetoceros* spp.) and the warmer oceanic water supported a much smaller biomass of relatively small single-celled species (e.g. small pennate diatoms, flagellates, coccolithophores, and dinoflagellates). Several factors, such as high nutrient concentrations, turbulence and upwelling circulation, and the proximity of the continental shelf, are responsible for diatom growth in coastal water [Barber et al., 1981; Smetacek, 1985]. These chain-forming cells do not grow well in the warmer, more stratified, nutrient-poor oceanic water where smaller flagellates dominate [Cushing, 1989].

The transition between these two biological zones was generally coincident with the front and the jet in our study area. Thus, the physical boundary delineated a biological boundary. Where the front (jet) extended seaward the diatom community extended seaward as well. Since most of the high phytoplankton biomass in the tongues and fila-

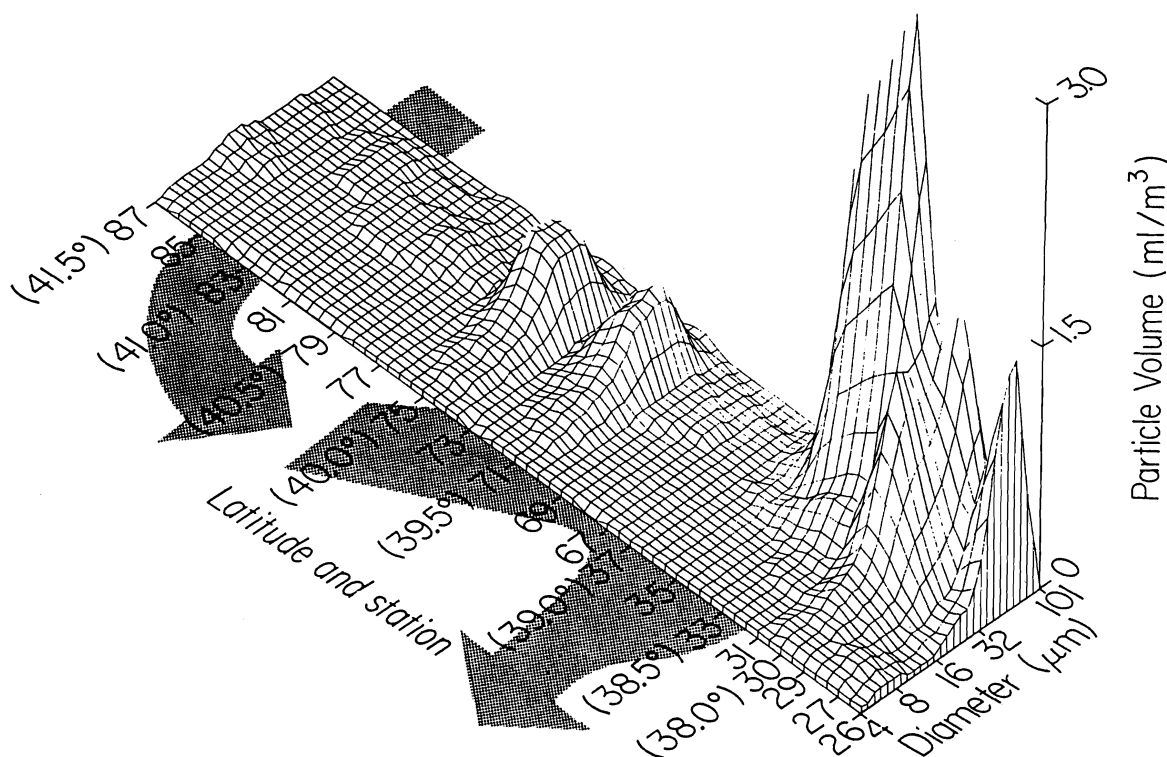


Fig. 10. An alongshore transect of the near-surface (5 m) distribution of estimated particle volume as a function of estimated particle size along station line II (see Figure 3). The grey-shaded arrows show the approximate locations of the jet crossings.

ments in our study area was associated with relatively slow moving water on the cold (low) side of the front (jet), we suggest that phytoplankton growth in these features was partly responsible for phytoplankton biomass observed there. Production rate measurements in the offshore diatom populations [Hood, 1990] show that these cells were capable of high photosynthetic rates. We believe that upwelling of nutrient-rich water associated with the geostrophic adjustment in the jet stimulated photosynthesis and biomass accumulation adjacent to it.

In the cold region, the biomass and species composition of the diatom community was quite variable. North of Cape Mendocino *Skeletonema costatum* and various *Chaetoceros* species were extremely abundant, but they were less abundant in the tongue of cold water that extended seaward off of Cape Mendocino. In this region, the diatom biomass was very patchy and several other diatom groups were numerous, such as *Rhizosolenia alata*, *Thalassiosira* spp. and *Nitzschia* spp.. In the cold water off Point Arena and Point Reyes, the diatom biomass was exceptionally high, largely due to the presence of large, single-celled, discoid *Actinocyclus* species, but the distribution of these diatoms was also extremely patchy. Along the southern portion of station line II (Figure 10) the diatom species composition changed from *Actinocyclus* spp. and *Rhizosolenia alata* dominance to *Skeletonema costatum* and *Chaetoceros* spp. dominance and then back again over a distance of less than 100 km. These spatial variations in the diatom species composition could have been a result of mixing of watermasses from different coastal regions which contained different phytoplankton populations, or they may reflect variations in the phytoplankton communities that developed around an upwelling

core south of the seaward-tilting jet off Point Arena [Margalef, 1978]. We suspect that both of these processes (mixing and growth) were responsible for the striking variations in the diatom species composition observed along the southern portion of station line II.

The negative log-linear relationship depicted in Figure 7 between chlorophyll concentration and dynamic height reflects the same physical and biological dynamics as the temperature and chlorophyll relationship. That is, the low sea surface heights were associated with cold, nutrient-rich, upwelled water which supported a high and variable biomass of diatom species, and the high sea surface heights were associated with warm, nutrient-poor water which supported a low and less variable biomass of smaller single-celled species. Thus, we interpret the relationship in Figure 7 spatially. That is, primarily as a reflection of the presence of two quasi-steady-state ecosystems, not as a reflection of the temporal decline in phytoplankton biomass which accompanies solar heating, nutrient depletion and grazing in upwelled water [Abbott and Zion, 1985].

So far in our discussion we have emphasized the large-scale patterns in temperature, flow, and phytoplankton biomass in our study area, and we have interpreted these patterns as a reflection of the presence of two distinct physical/biological regimes separated by a strong physical boundary. There is, however, evidence of entrainment and downstream advection of coastal water and coastal phytoplankters in the jet associated with this boundary. Figures 4 and 7 show that some relatively cold (down to 11.5°C), chlorophyll-rich (up to 4 mg m⁻³) surface water was being carried along the low side of the flow (between the 0.8 and 0.85 dyn m contours). And although Figure 8 shows

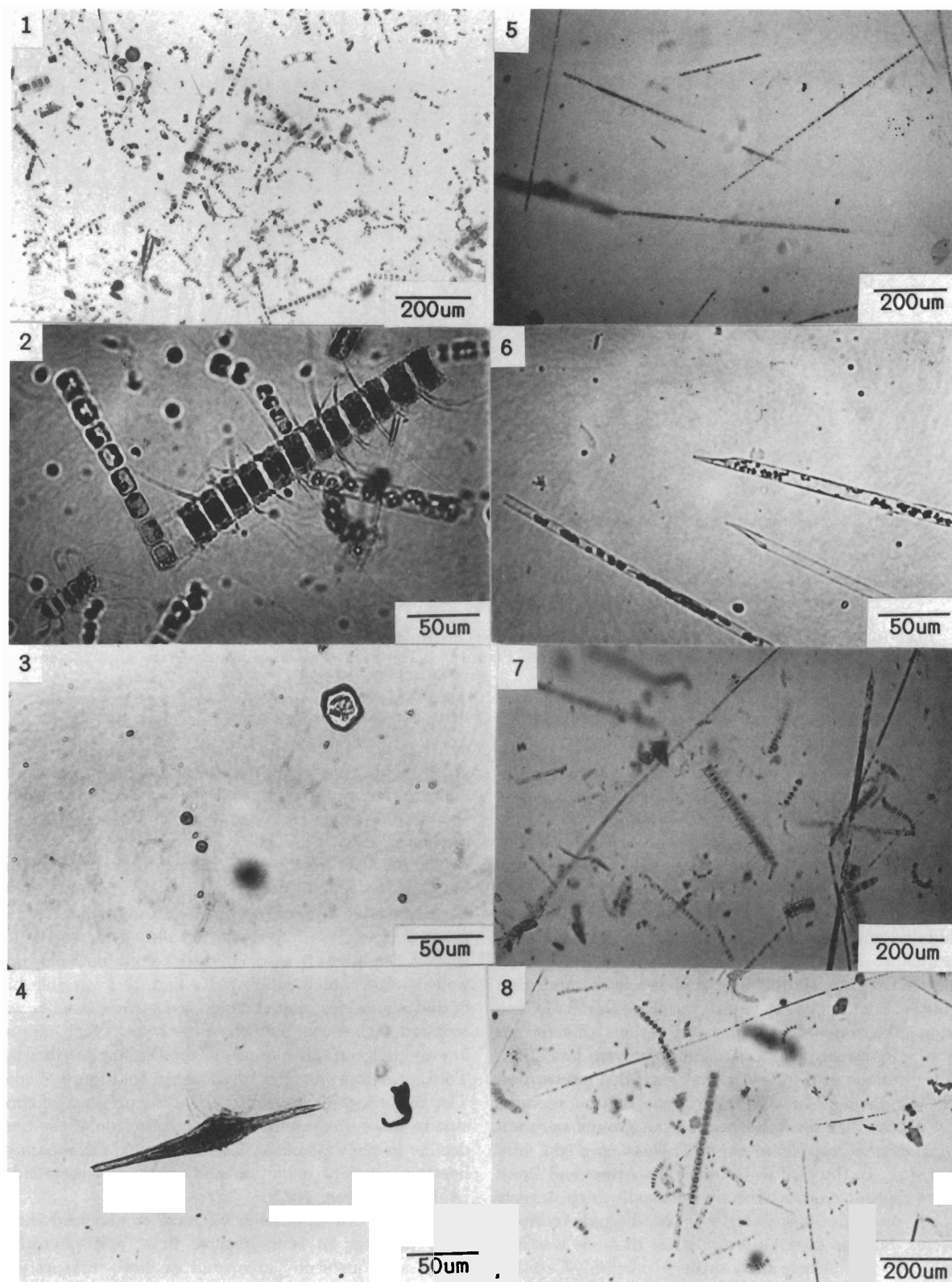


Fig. 11. Photomicrographs of near-surface (5 m) phytoplankton along station lines A and II. Frame 1: Station 123, mixed diatom assemblage dominated by *Chaetoceros* spp. and *Skeletonema costatum*. Frame 2: Station 123, closeup of *Chaetoceros costatus* and *Skeletonema wstatum*. Frame 3: Station 122, Small flagellates and particulates. Frame 4: Station 95, *Cemitium* sp.. Frame 5: Station 81, *Rhizosolenia alata*. Frame 6: Station 81, closeup of *Rhizosolenia alata*. Frame 7: Station 71, mixed diatom assemblage dominated by *Chaetoceros* spp., *Skeletonema wstatum*, and *Rhizosolenia alata*. Frame 8: Station 75, mixed diatom assemblage dominated by *Chaetoceros* spp., *Skeletonema wstatum*, and *Rhizosolenia alata*.

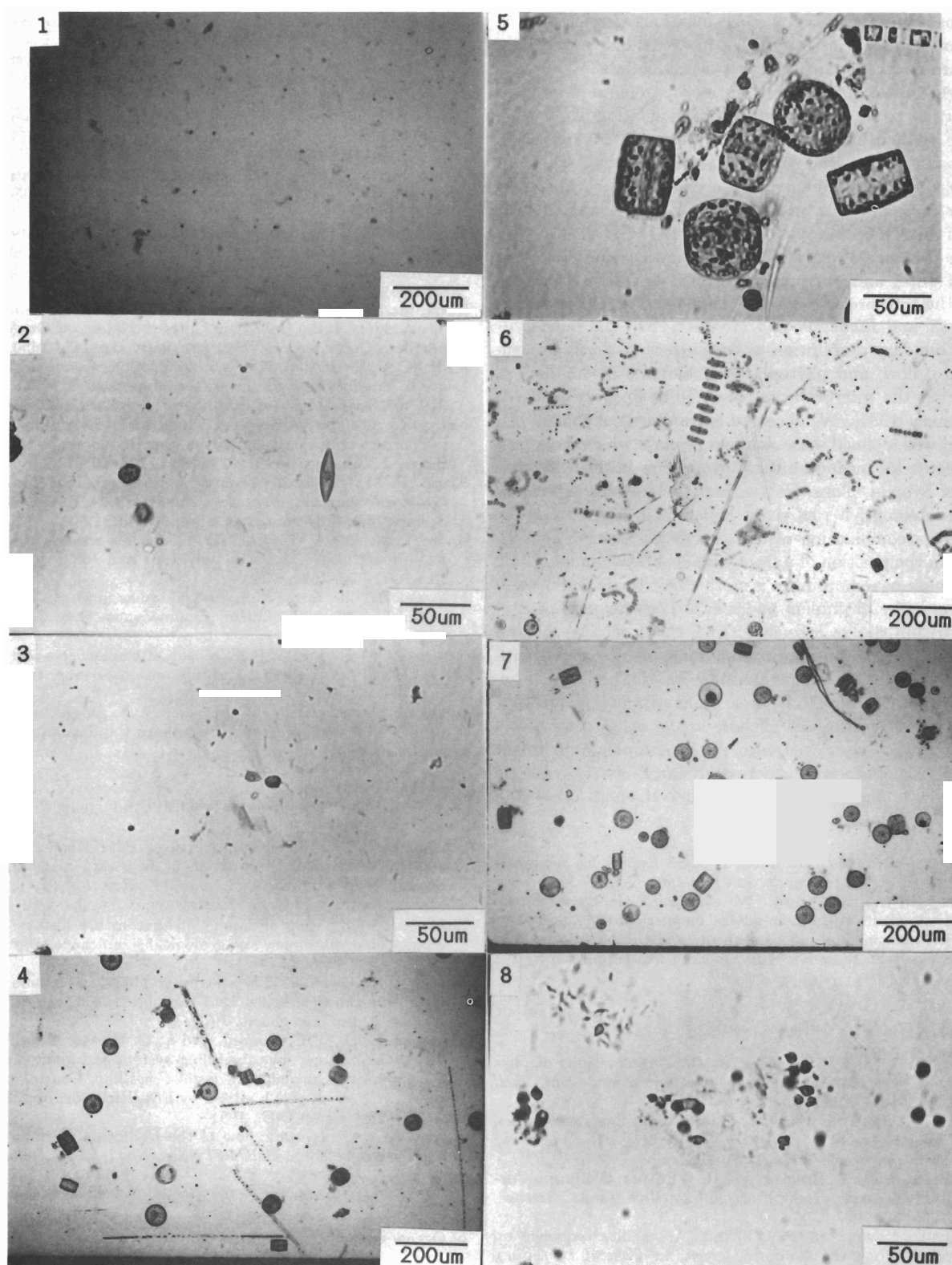


Fig. 12. Photomicrographs of near-surface (5 m) phytoplankton along station line II. Frame 1: Station 37, small, single-celled phytoplankters and particulates. Frame 2: Station 37, small pennate diatom and an armored dinoflagellate. Frame 3: Station 37, small single-celled flagellates. Frame 4: Station 33, diatom assemblage dominated by *Actinocyclus* spp. and *Rhizosolenia alata*. Frame 5: Station 33, closeup of *Actinocyclus* spp.. Frame 6: Station 30, mixed diatom assemblage dominated by *Chaetoceros* spp., *Skeletonema costatum*, *Thalassiosira* spp., and *Nitzschia* spp.. Frame 7: Station 26, *Actinocyclus* spp.. Frame 8: Station 26, small flagellates in a gelatinous matrix.

that the highest chlorophyll concentrations were associated with slow zonal flows, there are values in excess of 1 mg m^{-3} at eastward and westward velocities over 0.25 m s^{-1} . There is also evidence of entrainment and downstream advection in the particle data. The mixed diatom population responsible for the volume increase at station 71 in Figure 10 was in the jet where it flowed southeastward between Cape Mendocino and Point Arena, and the volume of *Rhizosolenia* and *Actinocyclus* cells was fairly high in the seaward flow at station 35 off Point Arena.

This evidence of entrainment and downstream advection of cold water and phytoplankton biomass in our data supports the interpretations of cold filaments in *Rienecker et al.* [1985] and *Rienecker and Mooers* [1989], and our large-scale boundary description of the surface patterns in temperature, flow, and phytoplankton biomass in our data is similar to the interpretation of satellite imagery in *Ikeda and Emery* [1984]. We observed entrainment of coastal water into well-defined seaward flows ("jets") which were part of a large-scale meandering southward flow in the California Current System. Thus, we interpret the seaward extensions of cold, chlorophyll-rich water apparent in our data as the result of a combination of two processes: alongshore variability in the position of a front that separated an upwelling water mass nearshore from a more oligotrophic water mass offshore, and entrainment and seaward advection of coastal water within the jet associated with this front. We believe that both vertical and horizontal transport associated with the meandering jet was responsible for the phytoplankton distributions in our study area. That is, it appears that cells were being advected offshore in the seaward flows and that upwelling associated with the geostrophic adjustment in the jet brought nutrient rich-deep water into the euphotic zone and stimulated phytoplankton growth on its low or cold side.

Acknowledgments. We thank Richard Eppley for reviewing and commenting on this work, and Elizabeth Venrick for her assistance with the microscopy. We also thank George Anderson and Dennis Gruber for their advice on methodology and their help with instruments and equipment, and the technicians and crew of the R.V. *Wecoma*. This research was supported by the Office of Naval Research.

REFERENCES

- Abbott, M. R., and P. M. Zion, Satellite observations of phytoplankton variability during an upwelling event, *Cont. Shelf Res.*, **4**, 661-680, 1985.
- Barber, R. T., and R. L. Smith, Coastal upwelling ecosystems, in *Analysis of Marine Ecosystems*, edited by A.R. Longhurst, pp. 31-68, Academic Press, N.Y., 1981.
- Bernstein, R. L., L. C. Breaker, and R. Whritner, California Current eddy formation: ship, air, and satellite results, *Science*, **195**, 353-359, 1977.
- Breaker, L. C., and R. P. Gilliland, A satellite sequence on upwelling along the California coast, in *Coastal Upwelling, Coastal and Estuarine Sciences*, vol. 1, edited by F.A. Richards, pp. 87-94, AGU, Washington D.C., 1981.
- Chelton, D. B., P. A. Bernal, and J. A. McGowan, Large-scale interannual physical and biological interaction in the California Current, *J. Mar. Res.*, **40**, 1095-1125, 1982.
- Coastal Transition Zone Group, The coastal transition zone program, *Eos Trans. AGU*, **69**, 698, 1988.
- Cushing, D. H., A difference in structure between ecosystems in strongly stratified waters and in those that are only weakly stratified, *J. Plankton Res.*, **11**, 1-13, 1989.
- Davis, R. E., Drifter observations of coastal surface currents during CODE: the method and the descriptive view, *J. Geophys. Res.*, **90**, 4741-4755, 1985.
- Flament, P., L. Armi, and L. Washburn, The evolving structure of an upwelling filament, *J. Geophys. Res.*, **90**, 11765-11778, 1985.
- Hood, R. R., Phytoplankton biomass, photosynthetic light response, and physical structure in a northern California upwelling system, Ph.D. thesis, 141 pp., Scripps Inst. of Oceanogr., La Jolla, Calif., 1990.
- Ikeda, M., and W. J. Emery, Satellite observations and modeling of meanders in the California Current System off Oregon and northern California, *J. Phys. Oceanogr.*, **14**, 1434-1450, 1984.
- Kelly, K. A., Swirls and plumes or application of statistical methods to satellite-derived sea surface temperatures, Ph.D. thesis, 210 pp., Scripps Inst. of Oceanogr., La Jolla, Calif., 1983.
- Kelly, K. A., The influence of winds and topography on the sea surface temperature patterns over the northern California Slope, *J. Gwphys. Res.*, **90**, 11783-11798, 1985.
- Kosro, P. M., Shipboard acoustic current profiling during the Coastal Ocean Dynamics Experiment, Ph.D. thesis, 119 pp., Scripps Inst. of Oceanogr., La Jolla, Calif., 1985.
- Kosro, P. M., and A. Huyer, CTD and velocity surveys of seaward jets off northern California, July 1981 and 1982, *J. Geophys. Res.*, **91**, 7680-7690, 1986.
- Margalef, R., Life-forms of phytoplankton as survival alternatives in an unstable environment, *Oceanologica Acta*, **1**, 493-509, 1978.
- Mooers, C. N. K., and A. R. Robinson, Turbulent jets and eddies in the California Current and inferred cross-shore transports, *Science*, **223**, 51-53, 1984.
- Rienecker, M. M., C. N. K. Mooers, D. E. Hagan, and A. L. Robinson, A cool anomaly off northern California: an investigation using IR imagery and in situ data, *J. Geophys. Res.*, **90**, 4807-4818, 1985.
- Rienecker, M. M., and C. N. K. Mooers, Mesoscale eddies, jets, and fronts off Point Arena, California, July 1986, *J. Geophys. Res.*, **94**, 12555-12569, 1989.
- Schramm, R. E., J. Fleischbein, A. Huyer, P. M. Kosro, T. Cowles and N. Dudek, CTD observations in the coastal transition zone off northern California, 9-18 June 1987, *Rep. 142*, 228 pp., College of Oceanogr., Oregon State Univ., Corvallis, OR., 1988.
- Smetacek, V. S., Role of sinking in diatom life-history cycles: ecological, evolutionary and geological significance, *Mar. Biol.*, **84**, 239-251, 1985.
- Smith, P. E., Distributional atlas of zooplankton volume in the California Current region, 1951 through 1966, *CalCOFI Atlas*, **No. 13**, 12 pp., 144 charts, 1971.
- Traganza, E. D., J. C. Conrad, and L. C. Breaker, Satellite observations of a cyclonic upwelling system and giant plume in the California Current, in *Coastal Upwelling, Coastal and Estuarine Sciences*, vol. 1, edited by F.A. Richards, pp. 228-241, AGU, Washington D.C., 1981.
- Wyllie, J.G., Geostrophic flow of the California Current at the surface and at 200m, *CalCOFI Atlas*, **No. 4**, 13 pp., 288 charts, 1966.

M. R. Abbott, R. R. Hood, A. Huyer and P. M. Kosro, College of Oceanography, Oregon State University, Corvallis, OR 97331.

(Received September 10, 1989;
accepted April 17, 1990.)